Some Theoretical Calculations of the Modern (e,2e) and (e,3e) Experiments

O. Chuluunbaatar, I.V. Puzynin,
Laboratory of Information Technologies, JINR
S.I. Vinitsky,
Bogoliubov Laboratory of Theoretical Physics, JINR
Yu.V. Popov, P.S. Vinitsky,
Nuclear Physics Institute, Moscow State University
B.B. Joulakian,
Laboratoire de Physique Moléculaire et des Collisions, France
Kh. Tsookhuu
National University of Mongolia, Mongolia

Аннотация

В работе [1] построены вариационные волновые функции основного состояния атома гелия для вычисления теоретических оценок сечения однократной и двухкратной ионизации и описания современных (e,2e), (e,3e) экспериментов. Построены волновые функции на экспоненциальном базисе удовлетворяющие условию Като (как в слабом так и в сильном смысле). Также построены параметрические асимптотические волновые функции непрерывного спектра кулоновской задачи двух центров [2]. В работах [3, 4] эти функции были использованы для вычисления теоретических оценок сечения однократной и двухкратной ионизации H_2 и N_2 для указанных выше экспериментов.

Pioneering theoretical calculations for the electron-helium double-ionization process where the scattered and two ejected electrons are detected in coincidence predicted a high sensitivity of the differential cross sections to the choices of initial- and final-state wave functions of the target. The first such experiment (e,3e) was performed by Lahmam-Bennani et al. [5] at small momentum transfer. The measurements were done on an absolute scale, which provides a stringent test for the models of the initial and final states of helium. Recently, Watanabe et al. [6] performed electron-helium double-ionization measurements at large momentum transfer and near the Bethe ridge, where the recoil momentum of the residual ion is small compared with the transferred momentum. In this experiment (e,3-1e) only the fast ejected electron is detected in coincidence with the scattered electron, while the slow ejected electron is undetected. In such kinematics the differential cross sections are primarily determined by the structure of the initial-state wave function, and hence we are lent a possibility to test various ground-state wave functions of helium. We might expect a better agreement with the above experiments if more specific features of electronic correlations are taken into account in the corresponding theoretical treatments. One of such features is Kato's cusp conditions, which are fulfilled by the exact wave function of helium in a configuration space.

The variational wave function is expanded in the form [1]

$$\Psi(r_1, r_2, r_{12}) = \sum_{i=1}^{N} D_i \left(\exp(-\alpha_i r_1 - \beta_i r_2) + \exp(-\alpha_i r_2 - \beta_i r_1)\right) \exp(-\gamma_i r_{12}) \qquad (1)$$

where α_i, β_i, and γ_i are real-valued parameters generated in a quasirandom manner at each integer i runs $1 \leq i \leq N$:

$$\begin{aligned}
\alpha_i &= \left\{\frac{1}{2} i(i+1)\sqrt{p_\alpha}\right\}(A_2 - A_1) + A_1, \quad 0 \leq A_1 < A_2, \\
\beta_i &= \left\{\frac{1}{2} i(i+1)\sqrt{p_\beta}\right\}(B_2 - B_1) + B_1, \quad 0 \leq B_1 < B_2, \\
\gamma_i &= \left\{\frac{1}{2} i(i+1)\sqrt{p_\gamma}\right\}(C_2 - C_1) + C_1, \quad 0 \leq C_1 < C_2.
\end{aligned} \tag{2}$$

Here $\{x\}$ is a fractional part of a real number x, p_α, p_β and p_γ are some prime numbers, $[A_1, A_2]$, $[B_1, B_2]$, and $[C_1, C_2]$ are real-valued variational intervals which need to be optimized. We use following the prime numbers set: $p_\alpha = 2$, $p_\beta = 3$ and $p_\gamma = 5$.

In principle, one can supplement the variational procedure with Kato's cusp conditions:

$$\frac{\frac{\partial \Psi(r_1,r_2,r_{12})}{\partial r_j}\Big|_{r_j \to 0}}{\Psi(r_1,r_2,r_{12})|_{r_j \to 0}} = -2, \quad j = 1,2, \quad \frac{\frac{\partial \Psi(r_1,r_2,r_{12})}{\partial r_{12}}\Big|_{r_{12} \to 0}}{\Psi(r_1,r_2,r_{12})|_{r_{12} \to 0}} = \frac{1}{2}. \tag{3}$$

However, this is extremely difficult to realize in practice, since in that case the wave function (1) should satisfy the two-particle cusp ratios locally—i.e., in every two-particle coalescence point of configuration space. Therefore we utilize in the variational procedure the averaged two-particle cusp ratios, which follow from Eq. (3) and traditionally occur in variational calculations

$$\begin{aligned}
\nu_j &= \frac{\left\langle \Psi(r_1,r_2,r_{12}) \middle| \delta(\mathbf{r_j}) \middle| \frac{\partial \Psi(r_1,r_2,r_{12})}{\partial r_1} \right\rangle}{\langle \Psi(r_1,r_2,r_{12}) | \delta(\mathbf{r_j}) | \Psi(r_1,r_2,r_{12}) \rangle} = -2, \quad j = 1,2, \\
\nu_{12} &= \frac{\left\langle \Psi(r_1,r_2,r_{12}) \middle| \delta(\mathbf{r_{12}}) \middle| \frac{\partial \Psi(r_1,r_2,r_{12})}{\partial r_{12}} \right\rangle}{\langle \Psi(r_1,r_2,r_{12}) | \delta(\mathbf{r_{12}}) | \Psi(r_1,r_2,r_{12}) \rangle} = \frac{1}{2}.
\end{aligned} \tag{4}$$

These two-particle cusp conditions can be regarded as "weak", since they are less stringent than those given by Eq. (3). The wave function satisfying the two-particle cusp conditions given by Eq. (4) will be referred to as 2PC. One can also derive from Kato's cusp conditions (3) the cusp ratios in the three-particle coalescence point. These are given by

$$\mu_1 = \mu_2 = \frac{\frac{\partial \Psi(r_1,r_2,r_{12})}{\partial r_1}\Big|_{r_1,r_2,r_{12} \to 0}}{\Psi(r_1,r_2,r_{12})|_{r_1,r_2,r_{12} \to 0}} = -2, \quad \mu_{12} = \frac{\frac{\partial \Psi(r_1,r_2,r_{12})}{\partial r_{12}}\Big|_{r_1,r_2,r_{12} \to 0}}{\Psi(r_1,r_2,r_{12})|_{r_1,r_2,r_{12} \to 0}} = \frac{1}{2}. \tag{5}$$

We will refer to the wave function satisfying these threeparticle cusp conditions as 3PC. In both cases the calculated cusp ratios for $N = 60$ are in good agreement with exact ones, $\nu_1 = \nu_2 = \mu_1 = \mu_2 = -2$ and $\nu_{12} = \mu_{12} = 0.5$, and yield the energy values E=-2.903 724 a.u. and E=-2.903 721 a.u., respectively (to seven significant digits the exact value is -2.903 724 a.u.).

Figure 1(a) shows the numerical results for the (e,3e) measurements performed by Lahmam-Bennani et al. [5]. In this setup all three outgoing electrons are detected in the same plane. The incident electron energy is E_i=5599 eV. The scattered electron energy and angle are E_s=5500 eV and $\theta_s = 0.45°$, respectively. The ejected electron energies are $E_a = E_b$ =10 eV. As can be seen, the 2PC and 3PC functions give almost identical results,

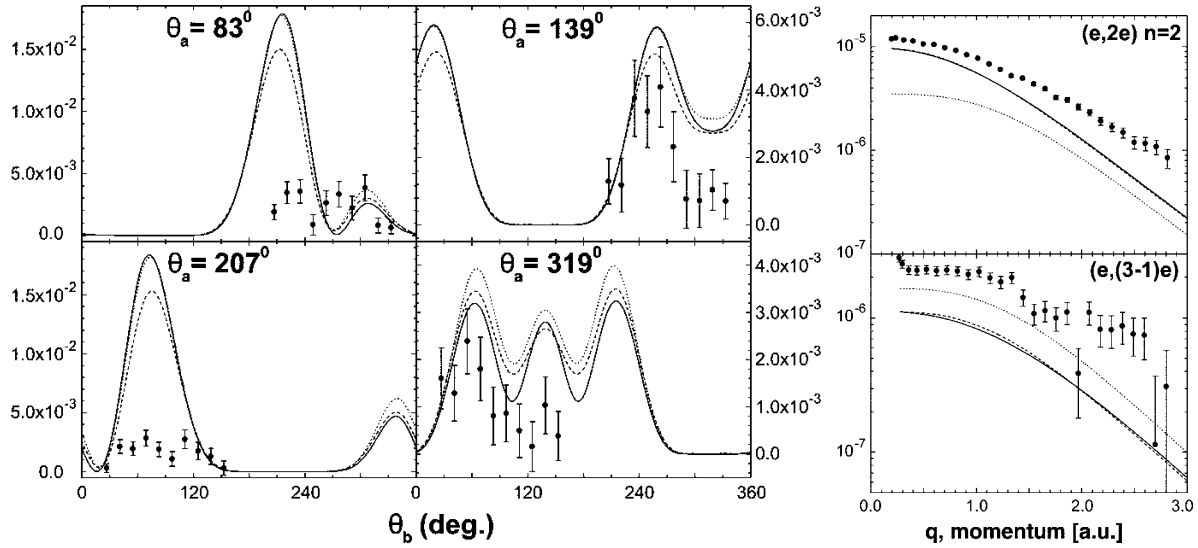

(a) (b)

Fig. 1: (a): Fivefold differential cross sections in atomic units of the (e,3e). Full dots with error bars correspond to experimental results of [5]. Theoretical curves are the results of the numerical calculations using the following wave functions of helium: 2PC (solid line), BK (dashed line), and Le Sech (dotted line). (b): The triple (upper panel) and fourfold (lower panel) differential cross sections in atomic units of the (e,2e) and (e,3-1e), respectively. Full dots with error bars correspond to experimental results of [6]. The curves are the results of PWIA calculations, convoluted with the experimental resolution function, using the following wave functions of helium: 2PC (solid line), BK (dashed line), and PL (dotted line)

which are visually indistinguishable and are very close to those using a Bonham and Kohl (BK) function [7]. Also are shown the results using the helium function by Le Sech (LS) [8]. Such a choice is motivated by the fact that the BK function gives a rather accurate energy value (E_{BK}=-2.9035 a.u.) but does not satisfy the cusp conditions even in the three-particle coalescence point, while the LS function exactly satisfies the cusp conditions in the three-particle coalescence point but gives a less accurate energy value (E_{LS}=-2.9020 a.u.). Figure 1(b) shows the numerical results for the recent symmetric noncoplanar (e,3-1e) and (e,2e) experiments by Watanabe et al. [6]. In these experiments two fast outgoing electrons, the scattered and ejected ones, having equal energies ($E_s = E_a$=1000 eV) and polar angles $\theta_s = \theta_a = 45°$ are detected. In the (e,3-1e) case, the slow ejected electron, which is not detected, has energy E_b=10 eV. The (e,2e) and (e,3-1e) cross sections are studied as functions of the momentum $\mathbf{q} = \mathbf{p_s} + \mathbf{p_a} - \mathbf{p_0}$. The calculations have been performed in the plane-wave impulse approximation (PWIA), and these results have been folded with the experimental momentum resolution. In the (e,3-1e) case the results using the 2PC and 3PC are very close to each other and also to those using the BK function. Interestingly, the Pluvinage (PL) function [7] better reproduces the (e,3-1e) experiment on an absolute scale, but it clearly fails in the case of (e,2e) transition to the n=2 excited state of He^+.

In paper [3], we studied theoretically the double ionization of H_2 by electron impact by describing the double electronic two center continuum by a product of two modified two-center Coulomb continuum (MTCC) [2] wave functions. This is particularly interesting, as the double continuum is constituted by two equivalent electrons coming from the electron cloud of the same target, in contrast to (e,2e) experiments, where only one of

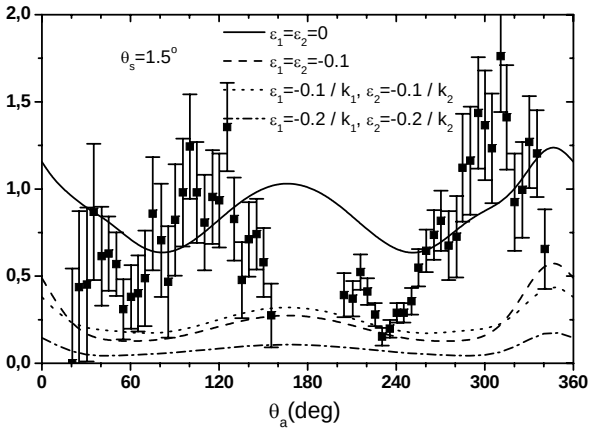

Fig. 2: The variation of fivefold differential cross section in atomic units of the (e,3-1e) with the ejection angle of electron having an energy of E_a=51 eV. The unobserved electron is the one having an energy of E_b=10 eV. The scattering angle $\theta_s = 1.5°$. Full squares with error bars correspond to experimental results of [9] scaled to the theory for the best visual fit at the binary lobe (around 300°)

the electrons comes from the target. This permits the verification of different theoretical models proposed to describe the electronic continuum and understand the mechanisms of the double ionization. Up to now, (e,3e) experiments have only been performed on atoms. Recently, (e,3-1e) experiments on molecular hydrogen at about 600 eV incident energy has been reported [9]. These experiments are double ionization experiments, where only one of the ejected electrons is detected in coincidence with the scattered electron. We have chosen as in the experiment of the Orsay group [9] an incident electron energy value of E_i=612 eV, ejection energy values of E_a=51 eV and E_b=10 eV respectively.

In figure 2 we observe that our method reproduces, for all the choices of small variational parameters ε_i of MTTC [2], the experimental structure of the variation of fivefold differential cross section in terms of the first ejection angle θ_a, with two maxima and two minima shifted with respect to the experimental curve. The theoretical results give all the same predominant direction parallel to momentum transfer $\mathbf{K}$ around $\theta_a = 350°$. The experimental curve seems to have been shifted. This disagreement of theory and experiment is also observed in simple ionization (e,2e) coincidence detection experiments, specially in the intermediate incidence energy regime. At higher incident energy values it disappear and both experiment and MTCC give similar results with the predominant ejection direction parallel to momentum transfer $\mathbf{K}$. Now the challenge for our theory is to explore the different improvements in the intermediate energy that we could introduce to try to match the theoretical results.

In paper [4], we studied theoretically the ionization of the nitrogen molecule, N_2, at large energy transfer using two center continuum (TCC) as particular case of MTTC. Figure 3(a) shows our measured triple differential cross sections distribution for ionization of the outermost orbitals of N_2, whereas figure 3(b) shows the similar results for ionization of the inner $^2\sigma_g$ orbital. Our data are compared on a relative scale with calculated results obtained using two state-of-the-art available approaches for molecular targets. The first one uses a first Born framework in which the TCC approximation with correct boundary conditions in the entrance and exit channels is applied. The second one is the molecular three body distorted wave (M3DW) approximation coupled with an orientation-averaged molecular orbital approximation (OAMO).

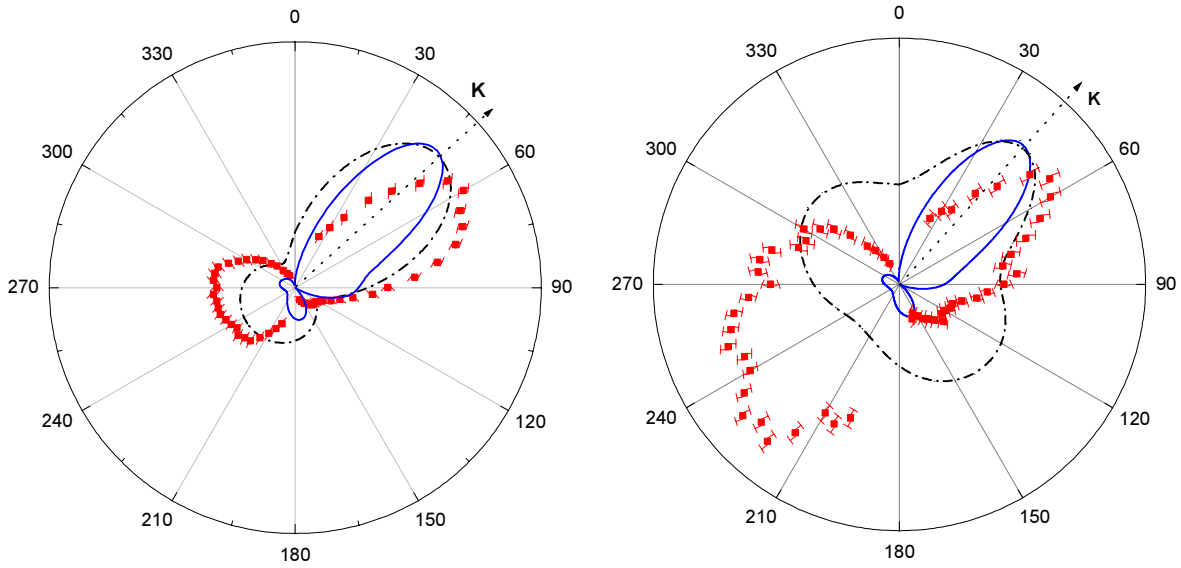

(a) (b)

Fig. 3: (a): Weighted sum of the triple differential cross section for ionization of N_2 from the $^3\sigma_g$, the $^1\sigma_u$ and the $^2\sigma_u$ 'outer' orbitals, at an incident electron energy $E_i = 589.6$ eV. The scattered electron with energy $E_s = 500$ eV is detected at an angle $\theta_a = 6°$ in coincidence with an emitted electron with energy $E_a = 74$ eV. The arrow indicates the momentum transfer direction ($\theta_K = 49°$). Full dots with error bars are the experimental data. Dash-dotted curve: theoretical predictions from the FBA-TCC model (weighted sum). Solid curve: theoretical predictions from the M3DW-OAMO model ($^3\sigma_g$ contribution only). Experiment and theories are all normalized for the best visual fit at the maximum of the binary lobe. (b): Same as in figure (a), but for the $^2\sigma_g$ 'inner' orbital at an incident electron energy $E_i = 612$ eV and $\theta_K = 43°$

References

[1] O. Chuluunbaatar, I.V. Puzynin, P.S. Vinitsky, Yu.V. Popov, K.A. Kouzakov and C. Dal Cappello, Phys. Rev. **A 74**, pp. 014703–1–4 (2006).

[2] O. Chuluunbaatar, B.B. Joulakian, Kh. Tsookhuu and S.I. Vinitsky, J. Phys. **B 37**, pp. 2607–2616 (2004).

[3] O. Chuluunbaatar, B.B. Joulakian, I.V. Puzynin, Kh. Tsookhuu and S.I. Vinitsky, accepted in J. Phys. **B** (2007).

[4] A. Naja, E.M. Staicu-Casagrande, A. Lahmam-Bennani, M. Nekkab, F. Mezdari, B. Joulakian, O. Chuluunbaatar and D.H. Madison, J. Phys. **B 40**, pp. 3775–3783 (2007).

[5] A. Lahmam-Bennani, I. Taouil, A. Duguet, M. Lecas, L. Avaldi and J. Berakdar, Phys. Rev. **A 59**, pp. 3548–3555 (1999).

[6] N. Watanabe, Y. Khajuria, M. Takahashi, Y. Udagawa, P.S. Vinitsky, Yu.V. Popov, O. Chuluunbaatar and K.A. Kouzakov, Phys. Rev. **A 72**, pp. 032705–1–11 (2005).

[7] L.U. Ancarani et al., Phys. Rev. **A 70**, pp. 012711–1–10 (2004).

[8] C. Le Sech, J. Phys. **B 30**, pp. L47–L50 (1997).

[9] A. Lahmam-Bennani, A. Duguet and S. Roussin, J. Phys. **B 35**, pp. L59–L63 (2002).